Ohta, M. and A. Takahashi. *Analysis Of Nuclear Transmutation Induced From Metal Plus Multibody-Fusion-Products, Reaction PowerPoint slides*. in *Tenth International Conference on Cold Fusion*. 2003. Cambridge, MA: LENR-CANR.org.

Slide 1

ANALYSIS OF NUCLEAR TRANSMUTATION INDUCED FROM METAL PLUS MULTIBODY-FUSION-PRODUCTS REACTION

* Masayuki OHTA
Akito TAKAHASHI

Department of Nuclear Engineering, Osaka University, JAPAN
* mohta@newjapan.nucl.eng.osaka-u.ac.jp

Slide 2

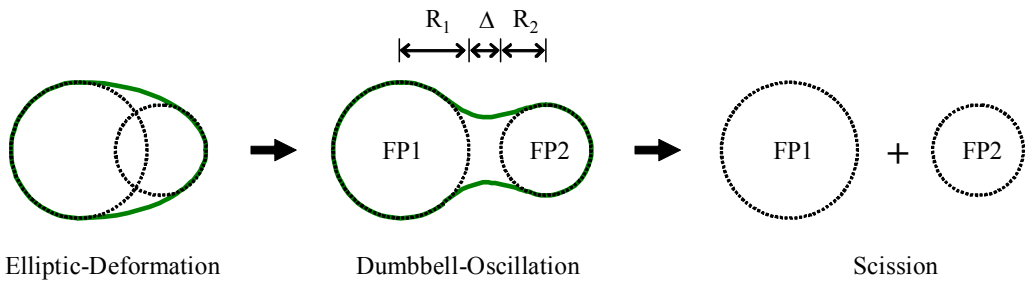

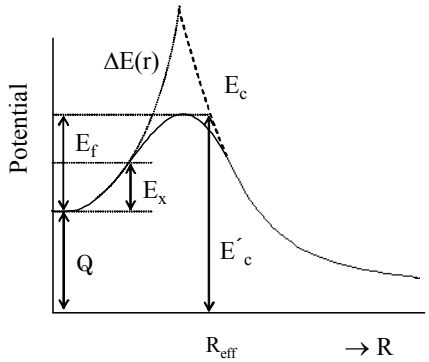

$E_c = 1.44\ Z_1 Z_2 / R$: Coulomb repulsion

$\Delta E(r) = \varepsilon(r)^2\ A^{2/3}\ (6.88 - 0.140\ Z^2/A)$

: Elliptic deform Energy

E'_c : Effective Coulomb Energy

E_x: Excitation Energy

E_f: Fission Barrier

$R_{eff} = \eta\,(R_1+R_2)$: Effecitve Scission Distance

Fig. 1-1: Fission process and potential

Slide 3

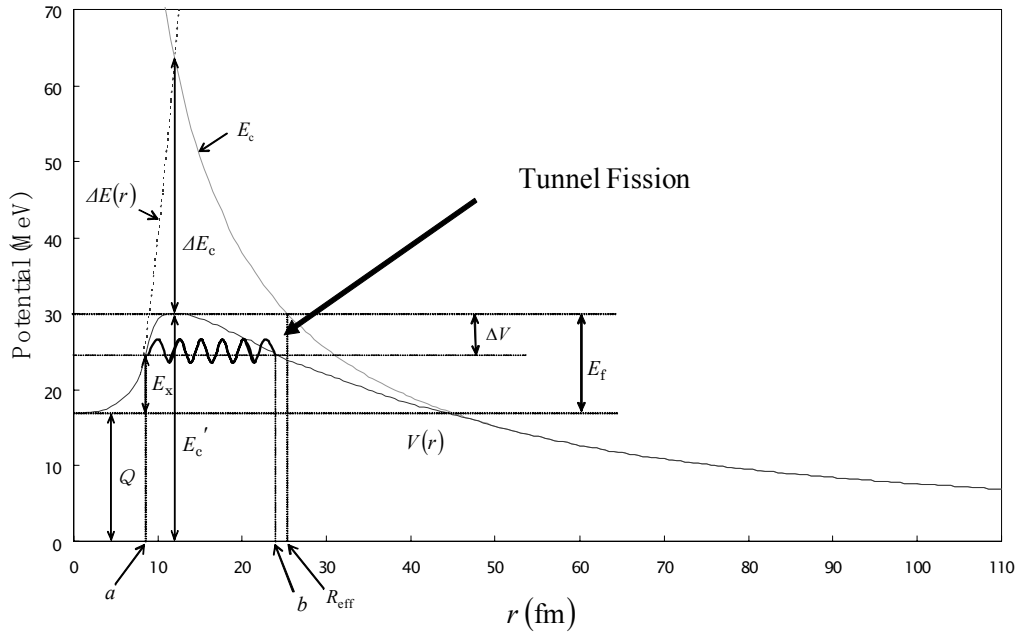

Fig. 1-2: Tunnel Fission

Slide 4

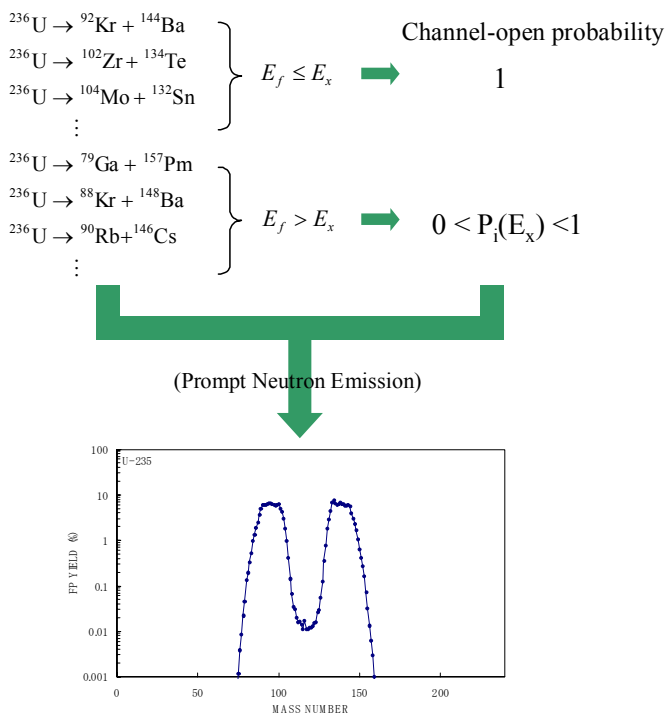

Fig. 1-3: Selective Channel Scission

Slide 5

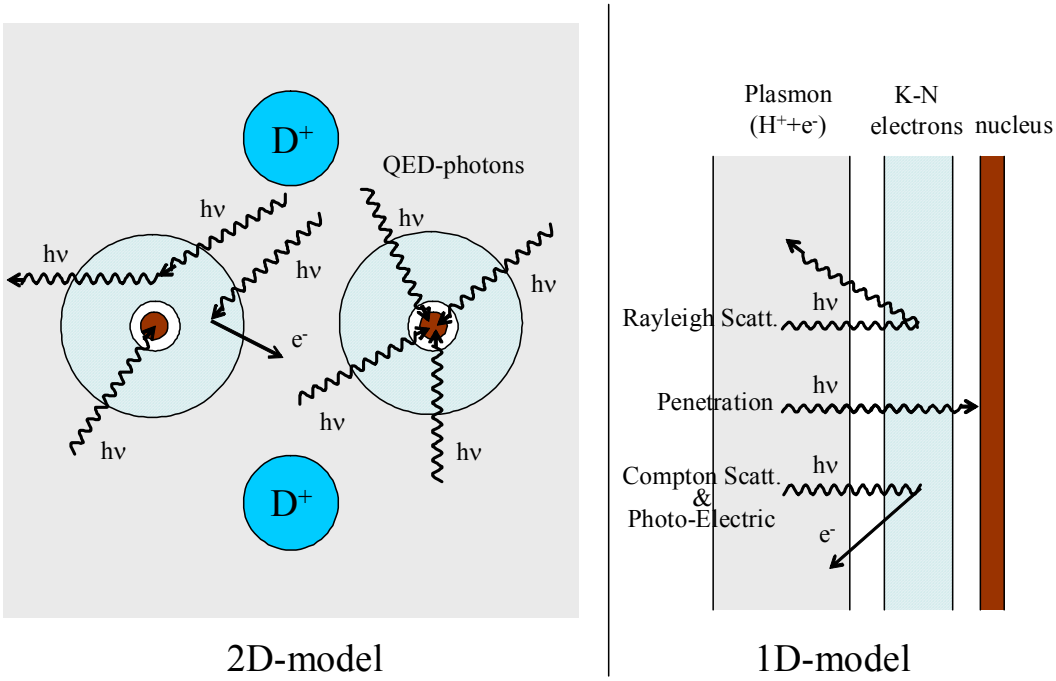

Fig. 2-1: Multi-Photon Absorption in Pd nucleus by QED Coupling to PdDx Plasma Oscillation

Slide 6

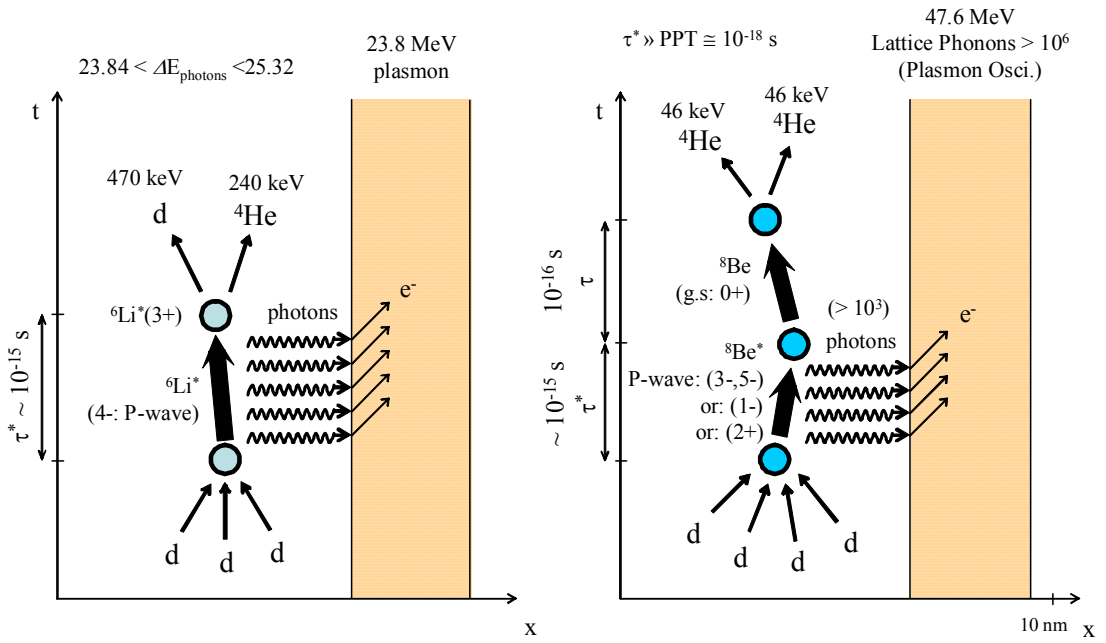

Fig. 2-2: Coherent X-rays for PdDx system

Slide 7

Multi-Photon Induced Fission Model

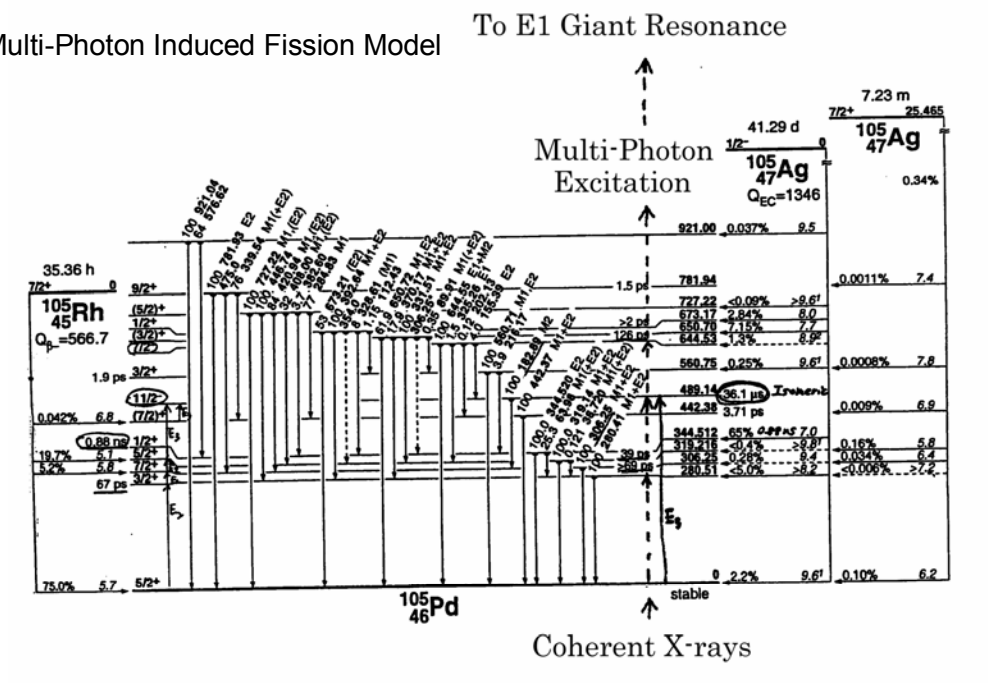

Fig. 2-3: Multi-Photon Excitation

Slide 8

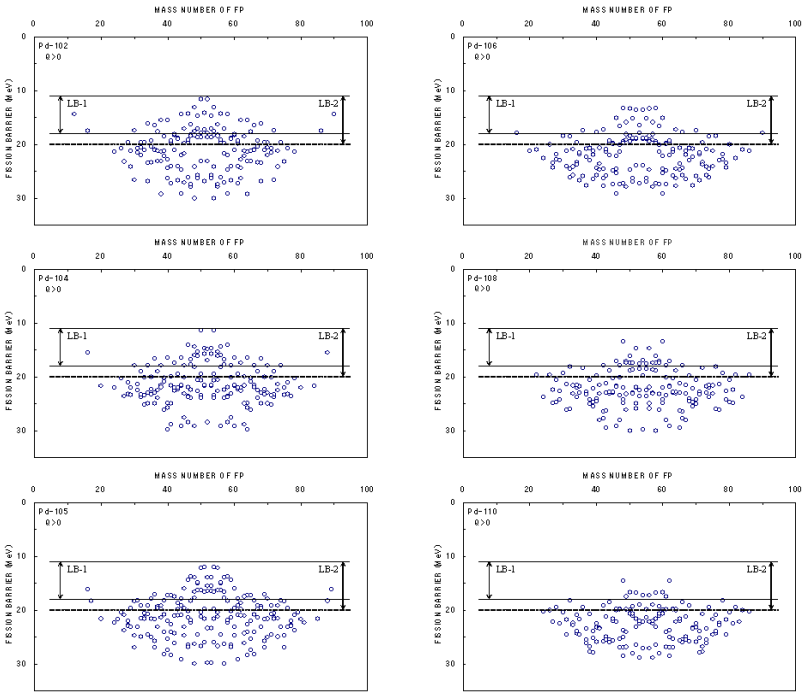

$_{46}$Pd	abundance(%)
102	1.02
104	11.14
105	22.33
106	27.33
108	26.46
110	11.72

Fig. 2-4: Fission barriers for Pd isotopes

Slide 9

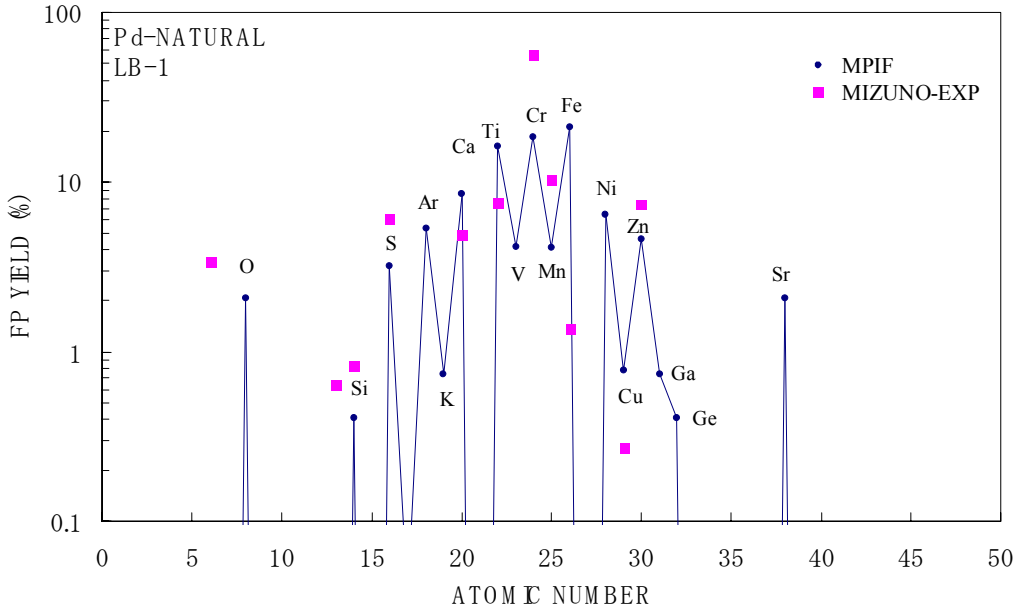

Fig. 2-5: Fission Product Yield for Atomic number (Pd photo-fission, LB-1 = 18 MeV)

Slide 10

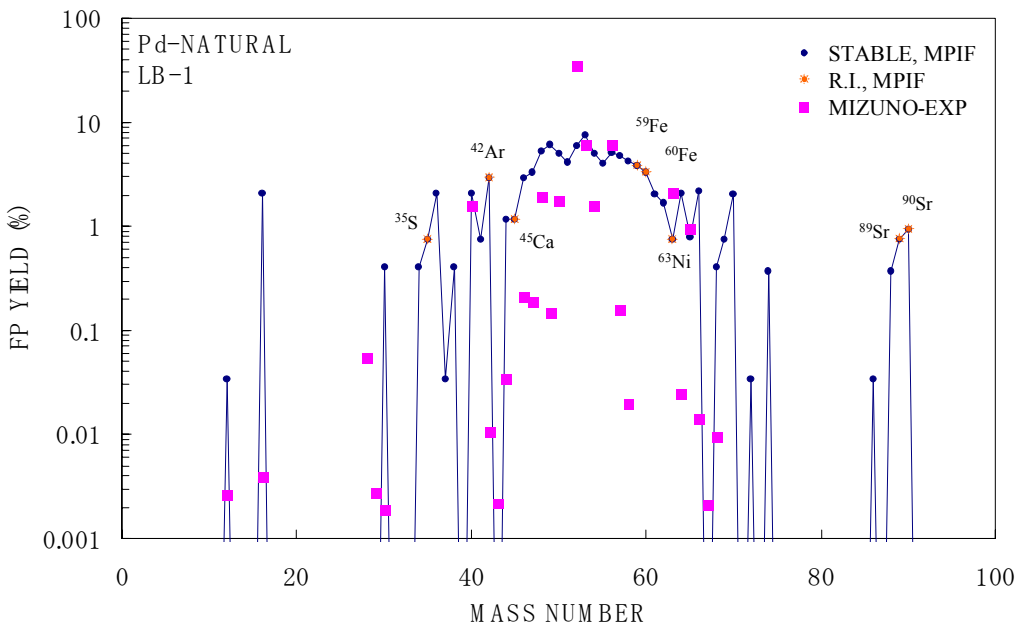

Fig. 2-6: Fission Product Yield for Mass number (Pd photo-fission, LB-1 = 18 MeV)

Slide 11

Nuclear Transmutation

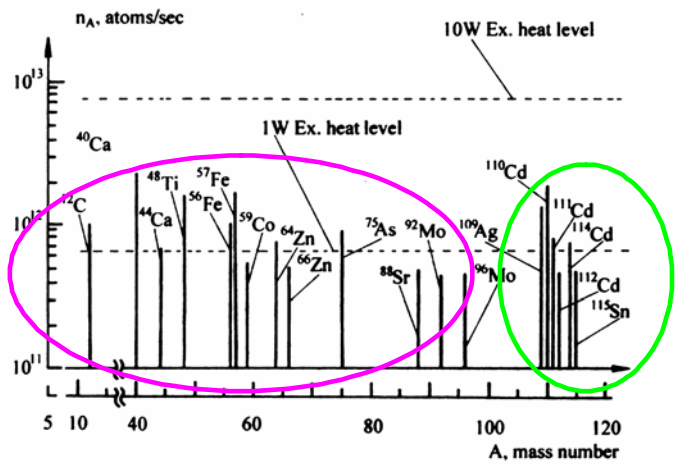

Fig.4. Impurity production rate in Pd cathode sample (near at the surface layer δ = 100 nm, d = 9 mm).

References:

A.B. Karabut, *Proc. ICCF9*, 151 (2002).

Slide 12

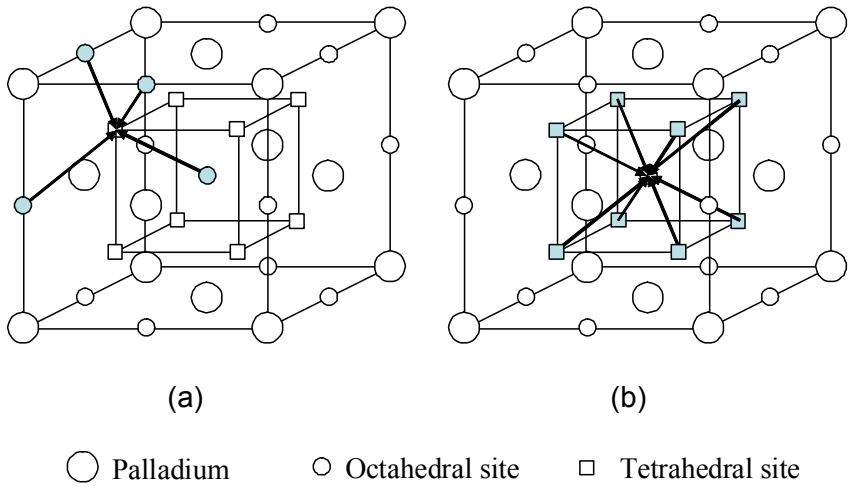

Fig. 3-1: 4D and 8D Fusions in Pd lattice

Slide 13

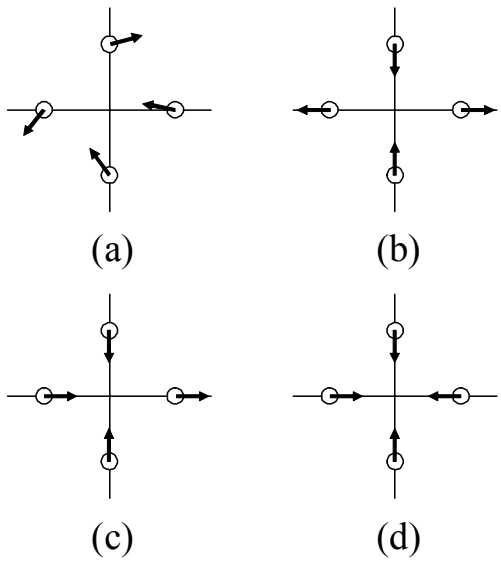

Fig. 3-2: Two-dimensional schematic view of coherent motion
(a) incoherent (b) anti-coherent (2D)
(c) coherent (3D) (d) coherent (4D)

Slide 14

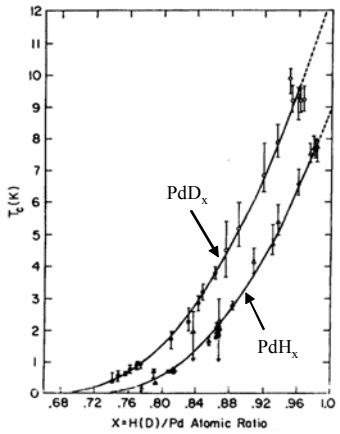

Fig. 3-3: Superconducting transition temperature as a function of H(D) concentrations for PdH$_x$ and PdD$_x$ [1)]

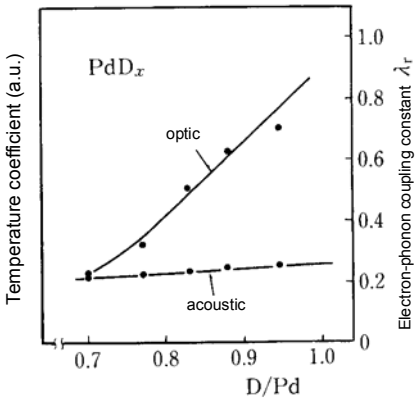

Fig. 3-4: Temperature coefficient of electric resistance for PdD$_x$ (acoustical and optical phonon mode) [2)]

electron-phonon interaction under transient condition

Enhancement of Screening Effect [3,4)]

References:

[1]: R.W. Standley, M. Steinback and C.B. Satterthwaite, "Superconductivity in PdHx(Dx) from 0.2 K to 4 K", *Solid State Commun*., **31**, 801 (1979).

[2]: J.P. Burger, Metal Hydrides, G. Bambakidis ed. (Plenum, 1981), p. 243.

[3]: A. Takahashi, "DRASTIC ENHANCEMENT OF D-CLUSTER FUSION BY ELECTRONIC QUASI-PARTICLE SCREENING ", *Proc. JCF4*, 74 (2002).

[4]: M. Ohta et al., "Possible Mechanism of Coherent Multibody Fusion", Proc. ICCF8, 403 (2000).

Slide 15

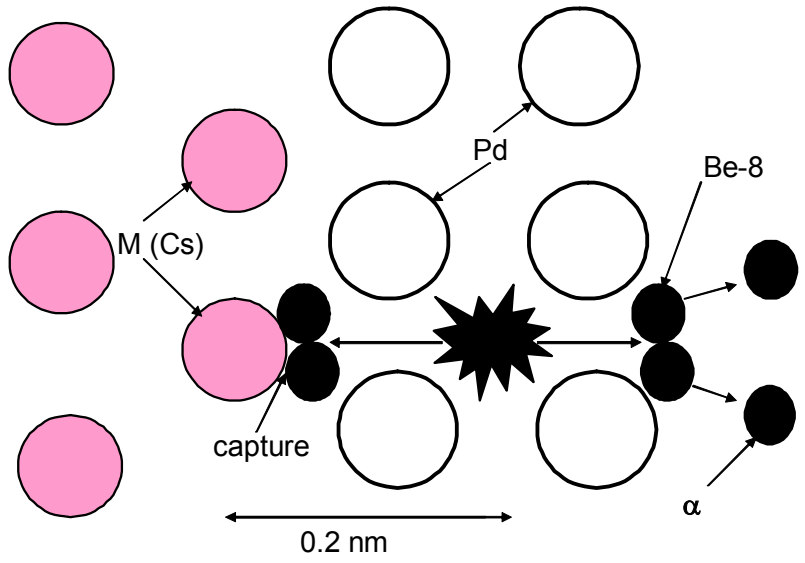

Fig. 3-5: 8D multi-body reaction

Slide 16

Multi-body Fusion Reaction

(1) 3D → $^{6}Li^{*}$ → d + ^{4}He + 23.8 MeV
(2) **4D → $^{8}Be^{*}$ → 2 ^{4}He + 47.6 MeV**
(3) **8D → $^{16}O^{*}$ (109.84 MeV) → 2 ^{8}Be + 95.2 MeV**
$^{8}Be^{*}$ → 2 ^{4}He + 47.6 MeV

4D and 8D Fusions can be selective. [1)]

References:
[1]: A. Takahashi, *Proc. JCF4*, 74 (2002).

Nuclear Transmutation

(1) **M + *Photons* → FP1 + FP2** (Ti, Cr, Fe etc.)

(2) **M + ^{4}He → M'** (Cd for Pd)
→ FP1' + FP2' (Ti, Cr, Fe etc.)

(3) **M + ^{8}Be → M''** (Sn for Pd, Pr for Cs, Mo for Sr)
→ FP1'' + FP2'' (Ti, Cr, Fe etc.)

Slide 17

Table 3-1: Natural abundance of Pd isotopes and

excitation energies of compound nucleus by + α and + ^{8}Be reactions

Nuclides	Natural abundance (%)	+ α (23.8 MeV)	Excitation energy (MeV)	+ ^{8}Be (47.6 MeV)	Excitation energy (MeV)
^{102}Pd	1.02	^{106}Cd*	25.4	^{110}Sn*	50.4
^{104}Pd	11.14	^{108}Cd*	26.1	^{112}Sn*	51.8
^{105}Pd	22.33	^{109}Cd*	26.3	^{113}Sn*	52.5
^{106}Pd	27.33	^{110}Cd*	26.7	^{114}Sn*	53.2
^{108}Pd	26.46	^{112}Cd*	27.3	^{116}Sn*	54.5
^{110}Pd	11.72	^{114}Cd*	27.9	^{118}Sn*	55.8

Slide 18

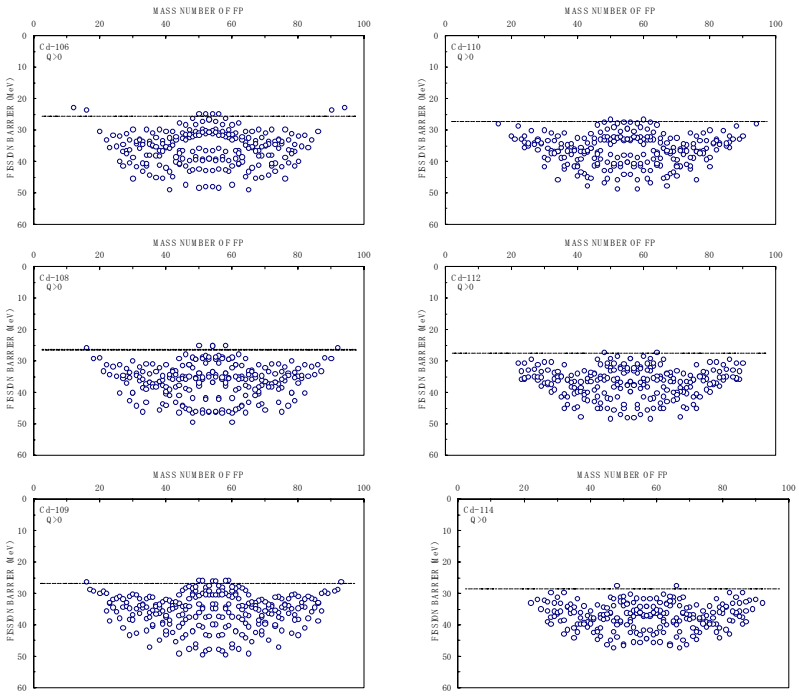

$_{48}$Cd	abundance(%)
106	1.02
108	11.14
109	22.33
110	27.33
112	26.46
114	11.72

Slide 19

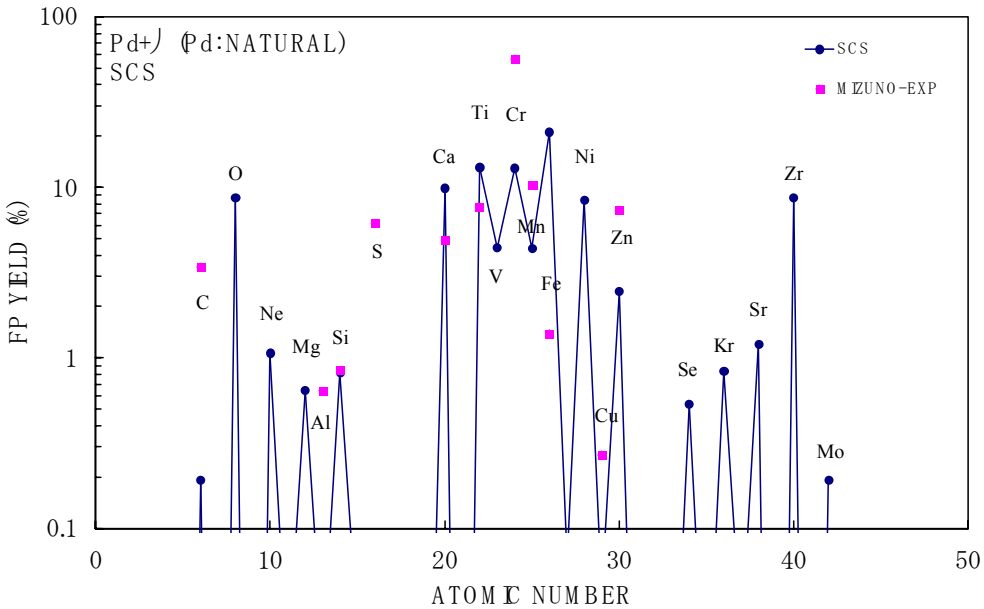

Fig. 4-7 :Fission Product Yield for Atomic number (Pd+α)

Slide 20

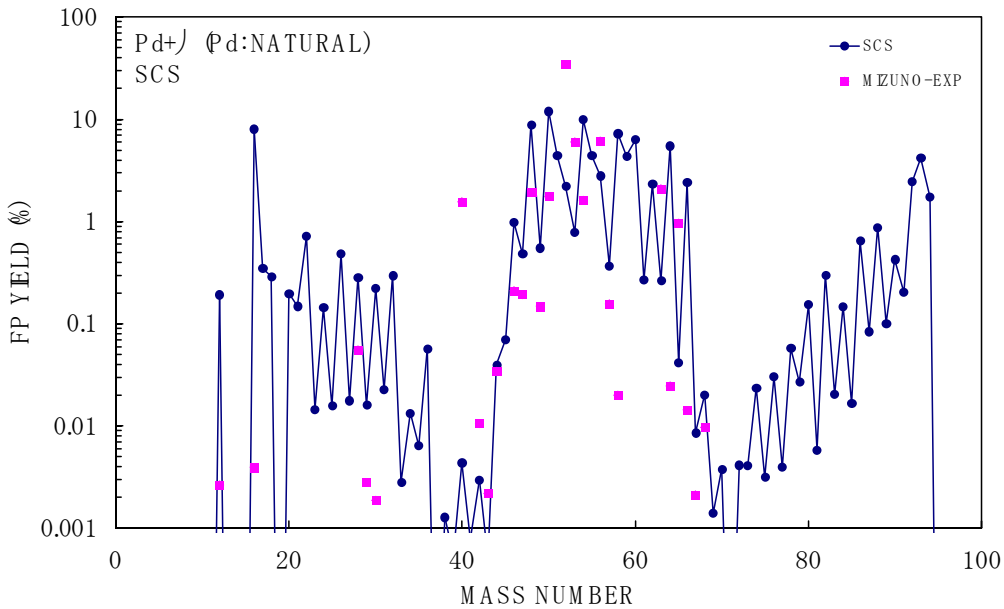

Fig. 4-8: Fission Product Yield for Mass number (Pd+α)

Slide 21

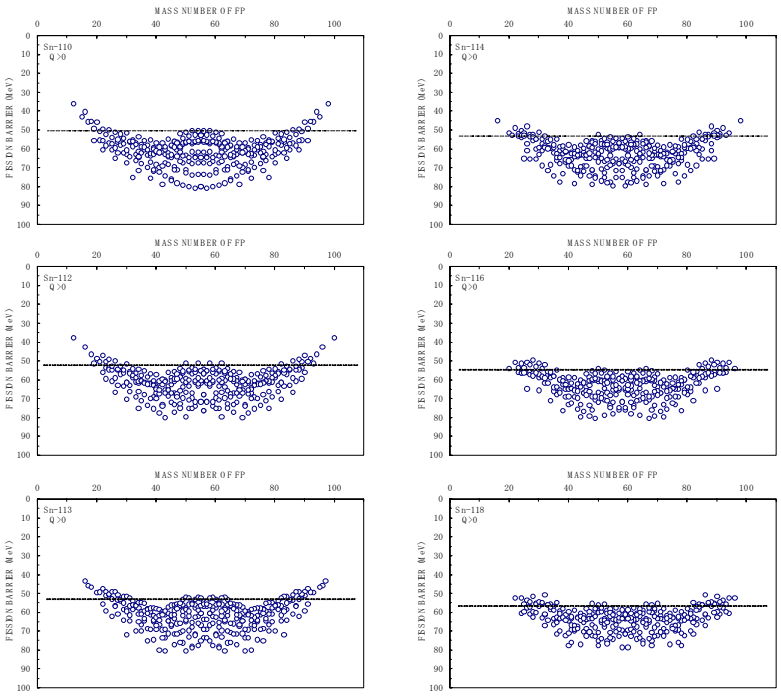

$_{48}$Sn	abundance(%)
110	1.02
112	11.14
113	22.33
114	27.33
116	26.46
118	11.72

Slide 22

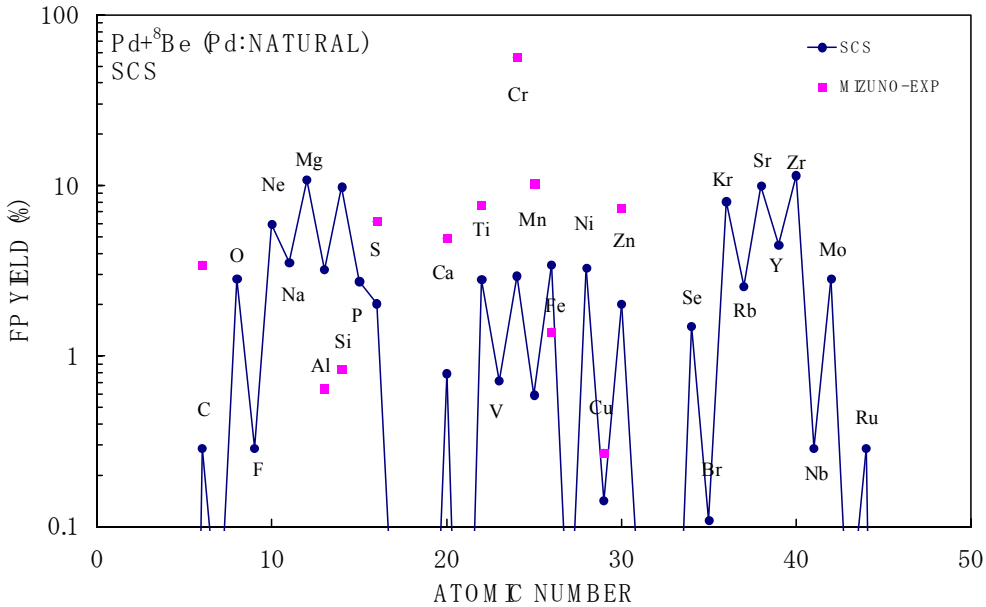

Fig. 5-7 :Fission Product Yield for Atomic number (Pd+^{8}Be)

Slide 23

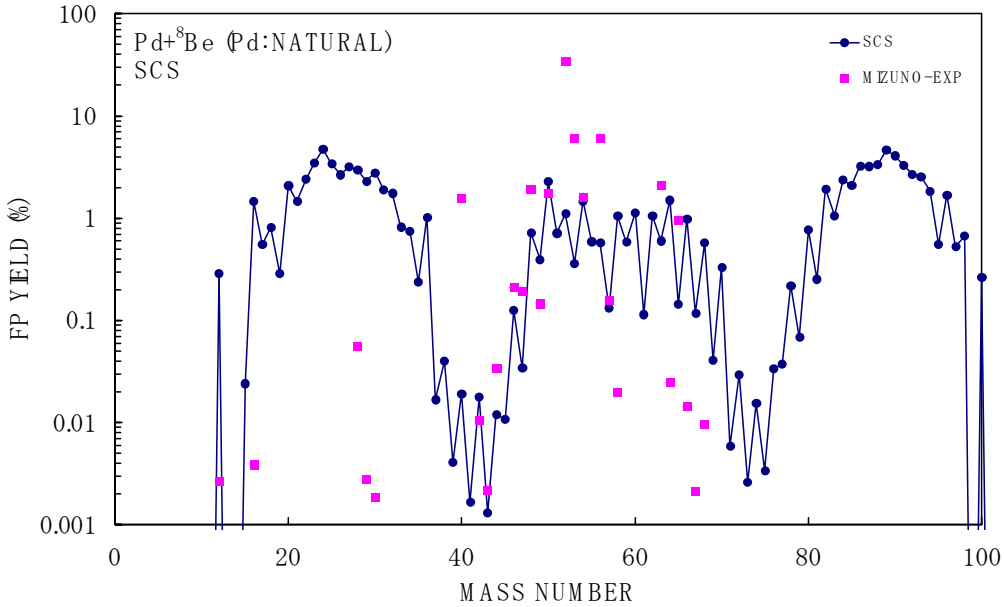

Fig. 5-8 :Fission Product Yield for Mass number (Pd+^{8}Be)

Slide 24

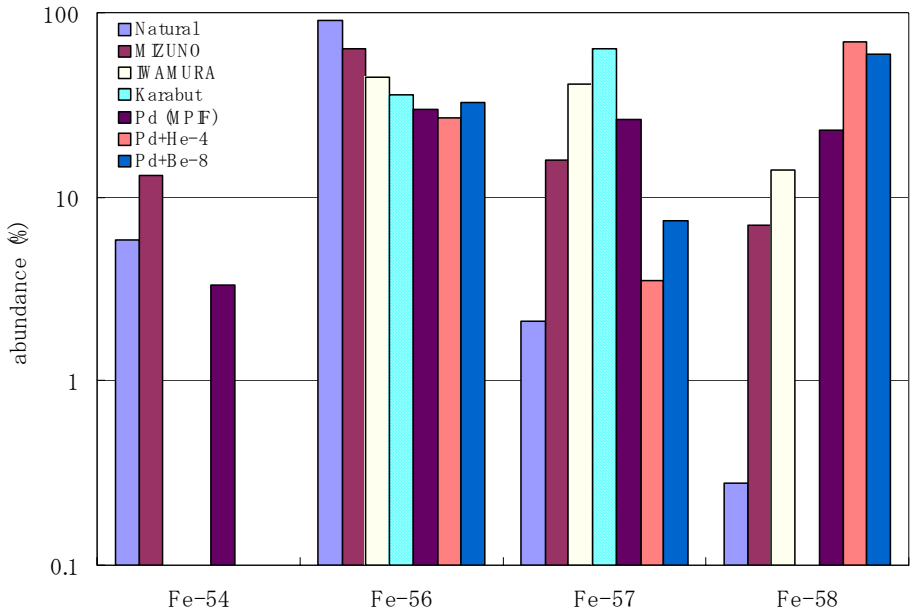

Fig. 6-1: Comparison of isotopic ratio between natural Fe, SCS analysis and experiments.

Slide 25

Discussion

Existence of $_{48}$Cd and $_{50}$Sn in some $_{46}$Pd-system experiment
Cs → Pr and Sr → Mo in Mitsubishi experiment

↓

Suggestion of Pd + α and Pd + ^{8}Be reactions

Nuclear transmutation (Production of Ti, Cr, Fe etc.)

↓

Suggestion of Fission
(Pd-photo fission or Pd + α or Pd + ^{8}Be ?)

Slide 26

Future work

Application of mode analysis
(*e.g.* U. Brosa et al., *Phys. Rep.* **197** (1990) 167.)

Analysis of γ-ray emission

Conclusion

Nuclear Transmutation was analyzed by Selective Channel Scission model.

- **M + *photons*** (*e.g.* A. Takahashi et al., *Proc.ICCF8* p.397)
- **M + ^{4}He**
- **M + ^{8}Be**

Slide 27

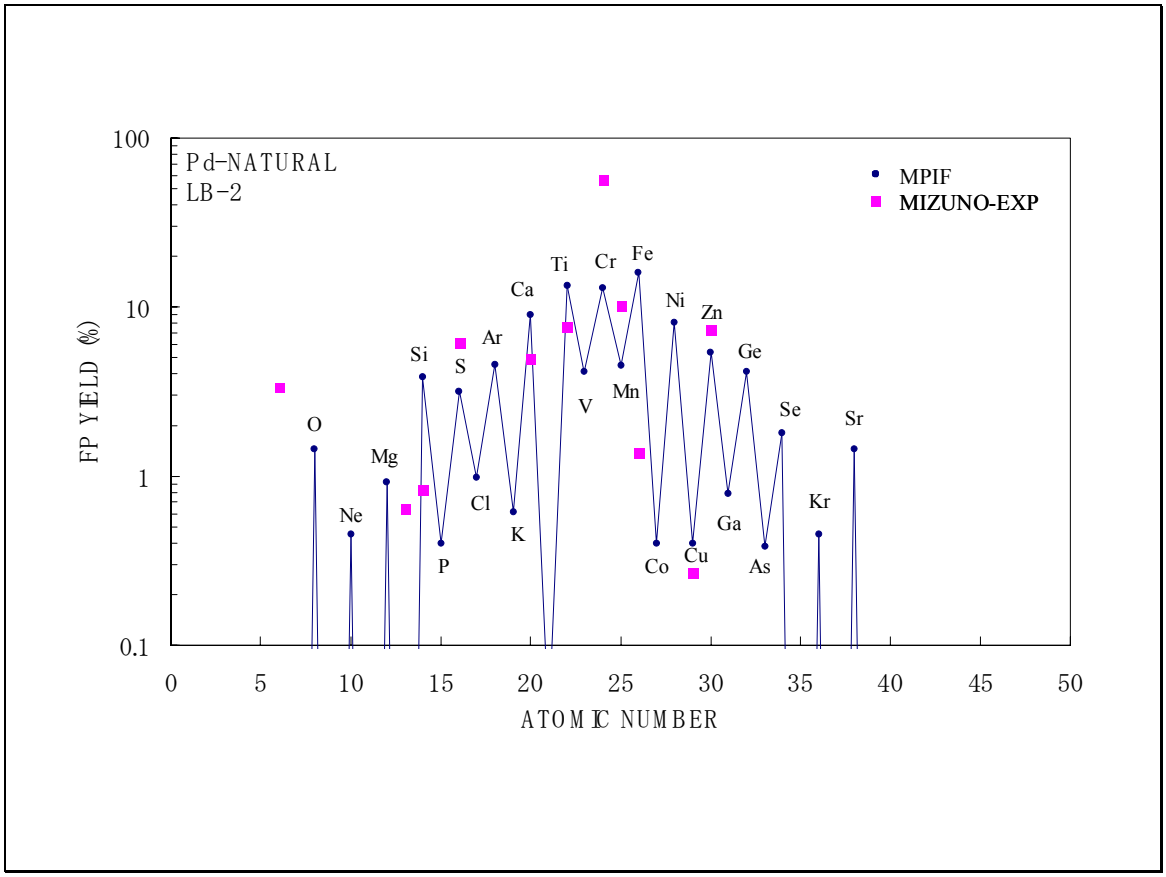
Pd-NATURAL
LB-2
MPIF
MIZUNO-EXP
FP YIELD (%)
ATOMIC NUMBER
100
10
1
0.1
0
5
10
15
20
25
30
35
40
45
50
O
Ne
Mg
Si
P
S
Cl
Ar
K
Ca
Ti
V
Cr
Mn
Fe
Co
Ni
Cu
Zn
Ga
Ge
As
Se
Kr
Sr

Slide 28

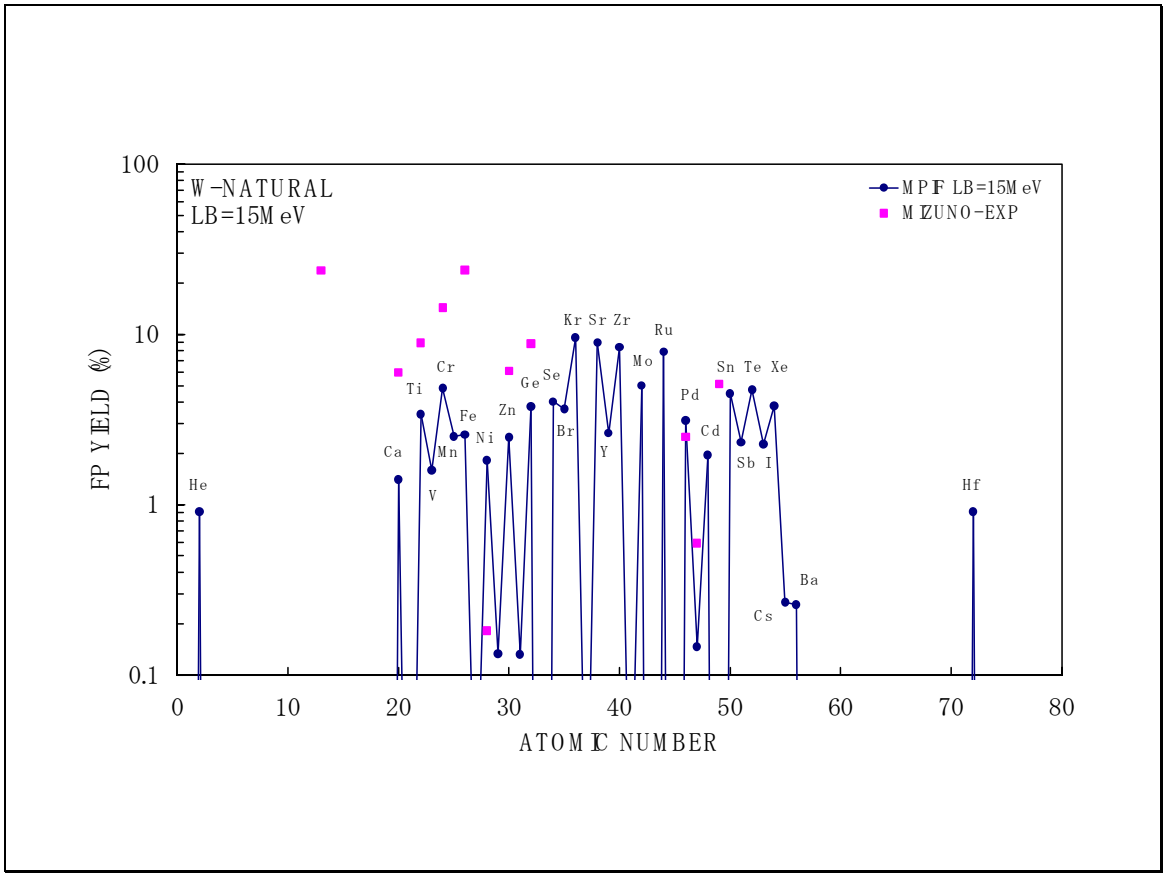
W-NATURAL
LB=15MeV
MPF LB=15MeV
MIZUNO-EXP
FP YIELD (%)
ATOMIC NUMBER
100
10
1
0.1
0
10
20
30
40
50
60
70
80
He
Ca
Ti
V
Cr
Mn
Fe
Ni
Zn
Ge
Se
Br
Kr
Sr
Y
Zr
Mo
Ru
Pd
Cd
Sn
Sb
Te
I
Xe
Cs
Ba
Hf

Slide 29

Table: Top 10 channel of Pd + α reaction

(1) $^{106}Cd \rightarrow {}^{12}C + {}^{94}Mo + 1.28$ MeV. ($E_f = 22.76$ MeV)

(2) $^{106}Cd \rightarrow {}^{16}O + {}^{90}Zr + 6.37$ MeV. ($E_f = 23.44$ MeV)

(3) $^{106}Cd \rightarrow {}^{50}Ti + {}^{56}Fe + 24.89$ MeV. ($E_f = 24.78$ MeV)

(4) $^{106}Cd \rightarrow {}^{52}Cr + {}^{54}Cr + 25.21$ MeV. ($E_f = 24.80$ MeV)

(5) $^{108}Cd \rightarrow {}^{50}Ti + {}^{58}Fe + 24.32$ MeV. ($E_f = 25.06$ MeV)

(6) $^{108}Cd \rightarrow {}^{54}Cr + {}^{54}Cr + 24.60$ MeV. ($E_f = 25.09$ MeV)

(7) $^{109}Cd \rightarrow {}^{50}Ti + {}^{59}Fe + 23.58$ MeV. ($E_f = 25.65$ MeV)

(8) $^{108}Cd \rightarrow {}^{16}O + {}^{92}Zr + 3.94$ MeV. ($E_f = 25.73$ MeV)

(9) $^{109}Cd \rightarrow {}^{51}Ti + {}^{58}Fe + 23.37$ MeV. ($E_f = 25.85$ MeV)

(10) $^{109}Cd \rightarrow {}^{54}Cr + {}^{55}Cr + 23.53$ MeV. ($E_f = 26.01$ MeV)

Slide 30

Table: Top 10 channel of Pd + ^{8}Be reaction

(1) $^{110}Sn \rightarrow {}^{12}C + {}^{98}Ru + 2.39$ MeV. ($E_f = 35.87$ MeV)

(2) $^{112}Sn \rightarrow {}^{12}C + {}^{100}Ru + 0.56$ MeV. ($E_f = 37.53$ MeV)

(3) $^{110}Sn \rightarrow {}^{16}O + {}^{94}Mo + 7.31$ MeV. ($E_f = 40.23$ MeV)

(4) $^{112}Sn \rightarrow {}^{16}O + {}^{96}Mo + 4.87$ MeV. ($E_f = 42.46$ MeV)

(5) $^{110}Sn \rightarrow {}^{15}N + {}^{95}Tc + 0.08$ MeV. ($E_f = 42.74$ MeV)

(6) $^{113}Sn \rightarrow {}^{16}O + {}^{97}Mo + 3.95$ MeV. ($E_f = 43.28$ MeV)

(7) $^{114}Sn \rightarrow {}^{16}O + {}^{98}Mo + 2.29$ MeV. ($E_f = 44.83$ MeV)

(8) $^{110}Sn \rightarrow {}^{18}O + {}^{92}Mo + 1.75$ MeV. ($E_f = 45.34$ MeV)

(9) $^{110}Sn \rightarrow {}^{17}O + {}^{93}Mo + 1.78$ MeV. ($E_f = 45.53$ MeV)

(10) $^{110}Sn \rightarrow {}^{20}Ne + {}^{90}Zr + 9.98$ MeV. ($E_f = 45.61$ MeV)

Slide 31

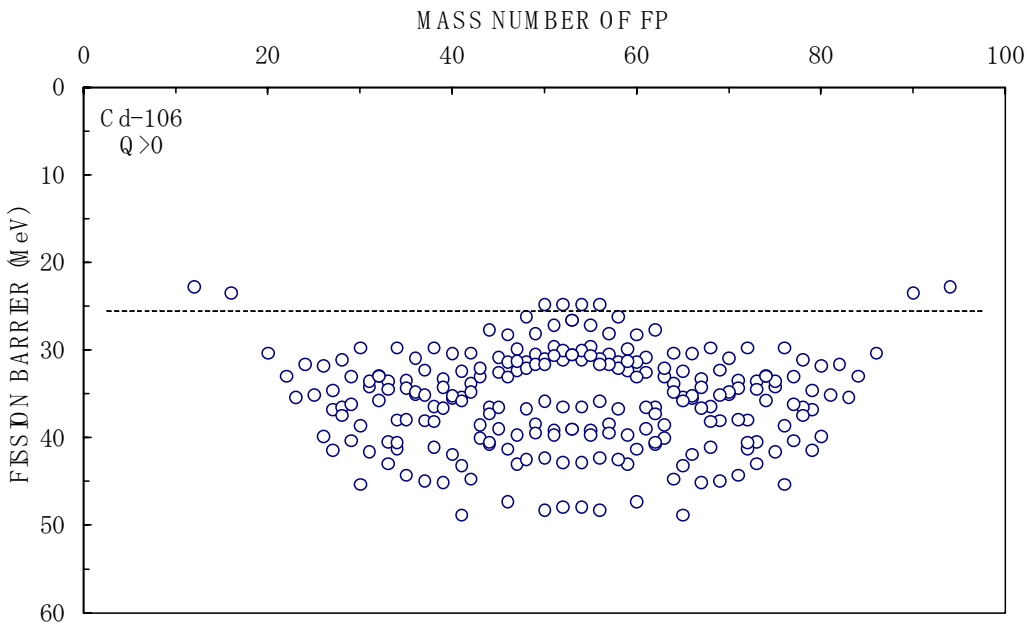

Fig. 4-1: Fission barriers for Cd-106

Slide 32

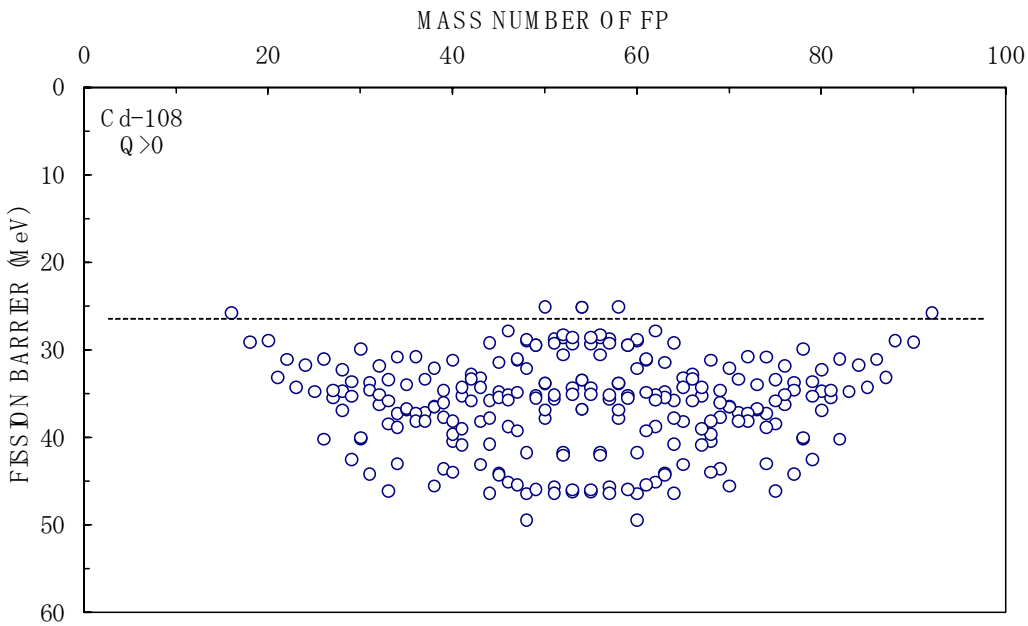

Fig. 4-2: Fission barriers for Cd-108

Slide 33

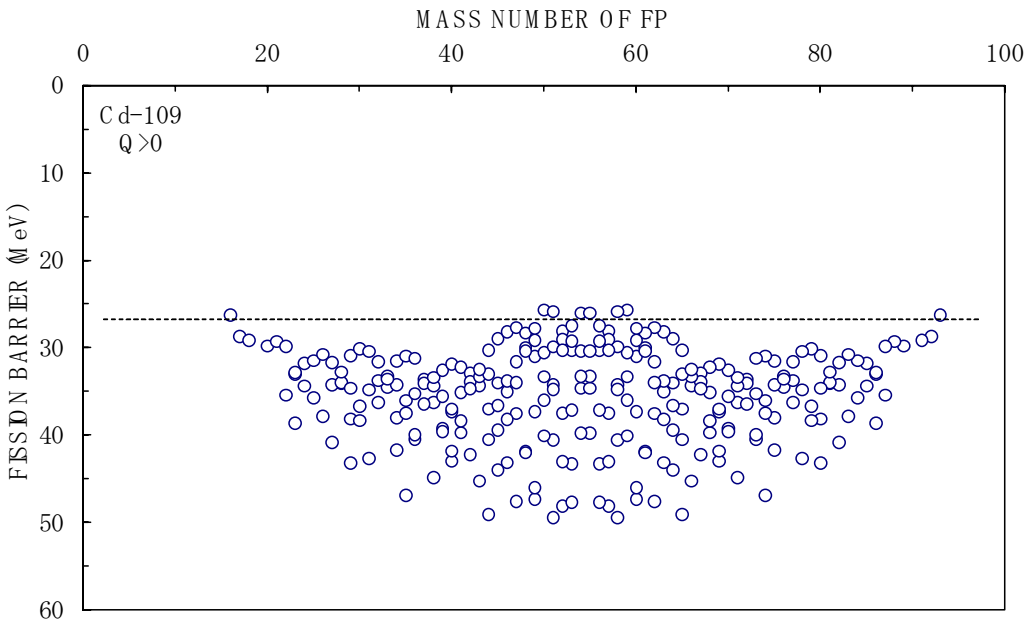

Fig. 4-3: Fission barriers for Cd-109

Slide 34

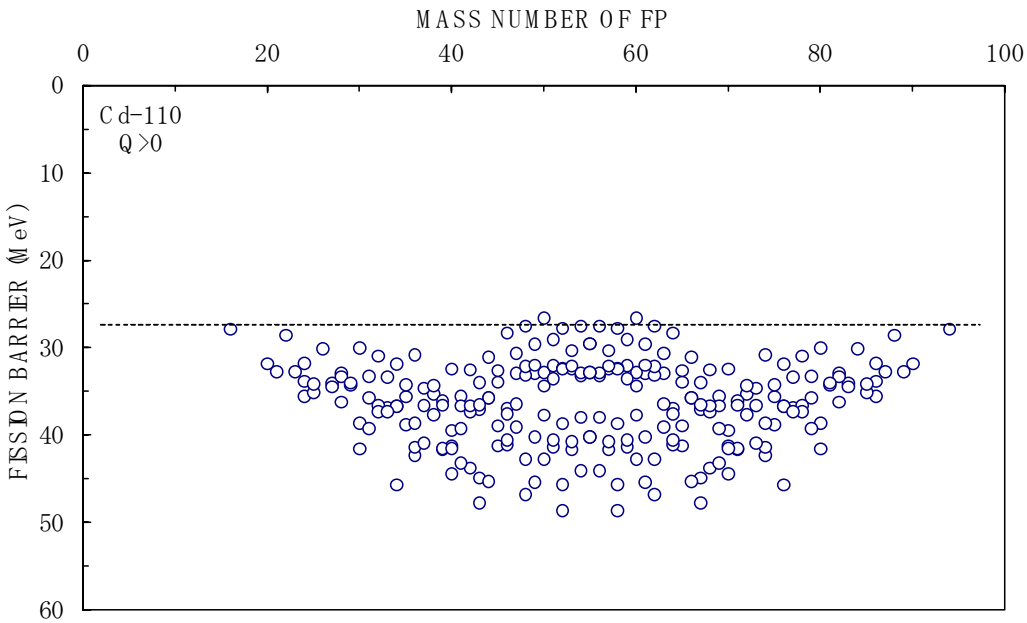

Fig. 4-4: Fission barriers for Cd-110

Slide 35

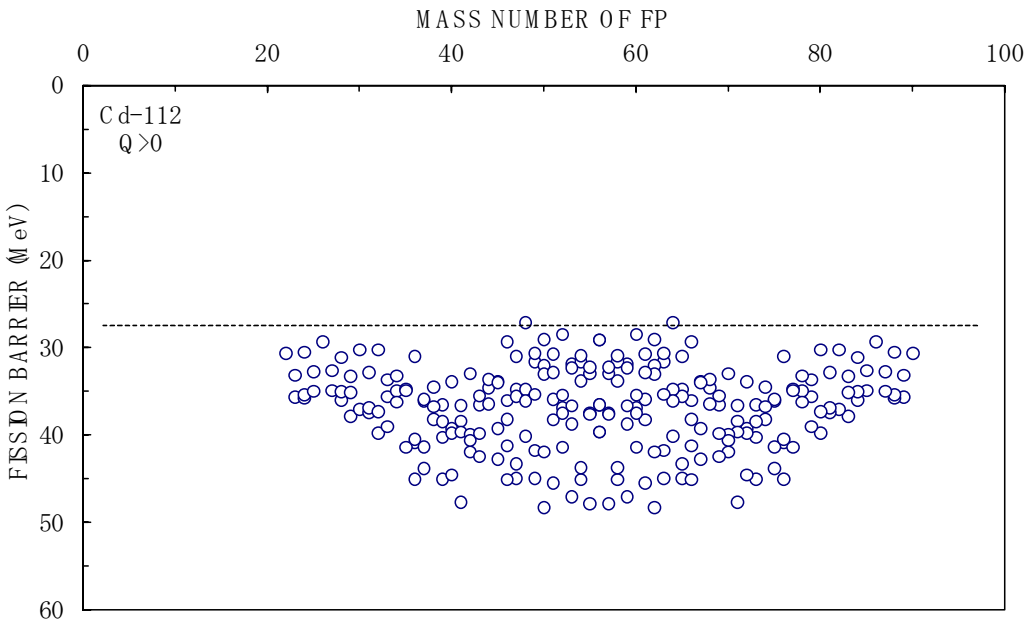

Fig. 4-5: Fission barriers for Cd-112

Slide 36

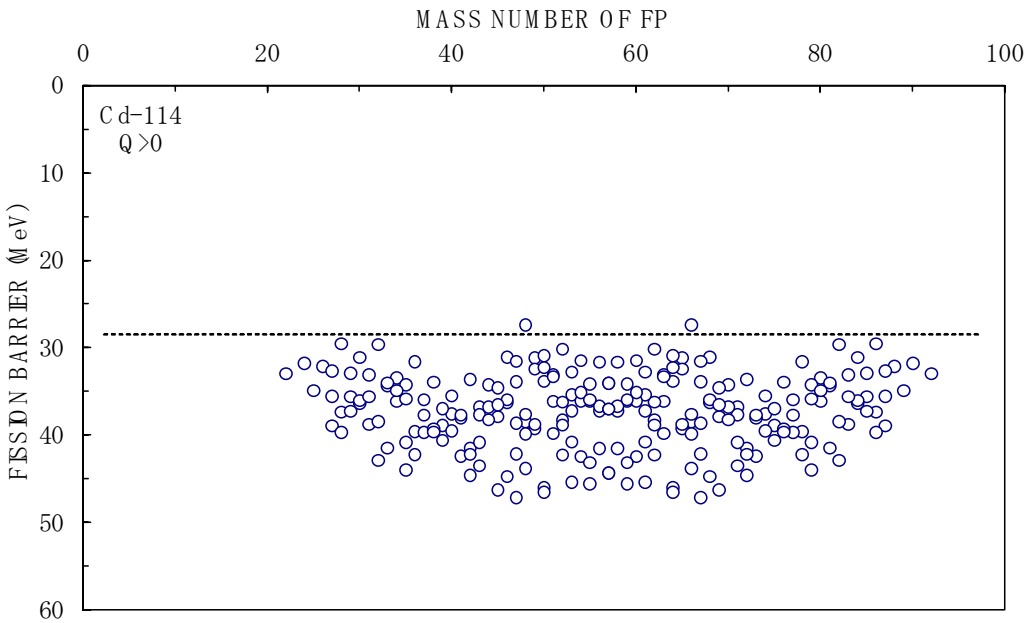

Fig. 4-6: Fission barriers for Cd-114

Slide 37

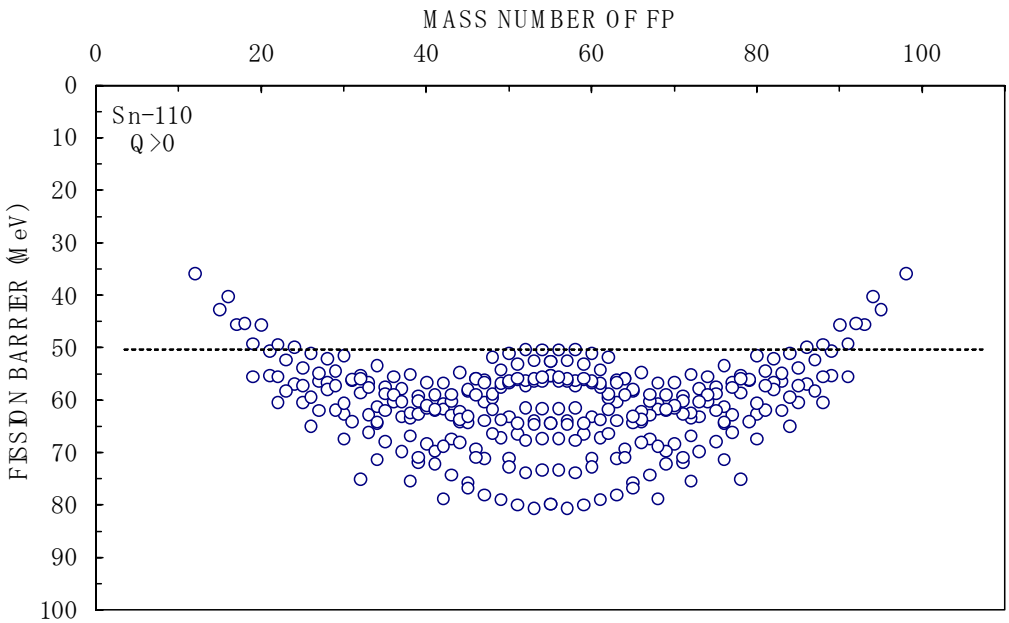

Fig. 5-1: Fission barriers for Sn-110

Slide 38

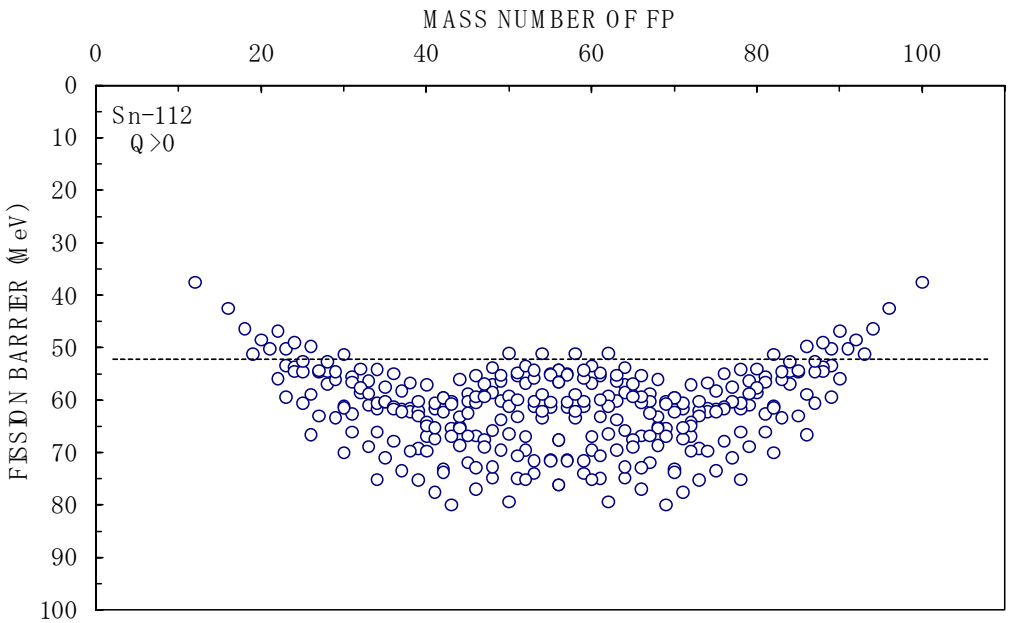

Fig. 5-2: Fission barriers for Sn-112

Slide 39

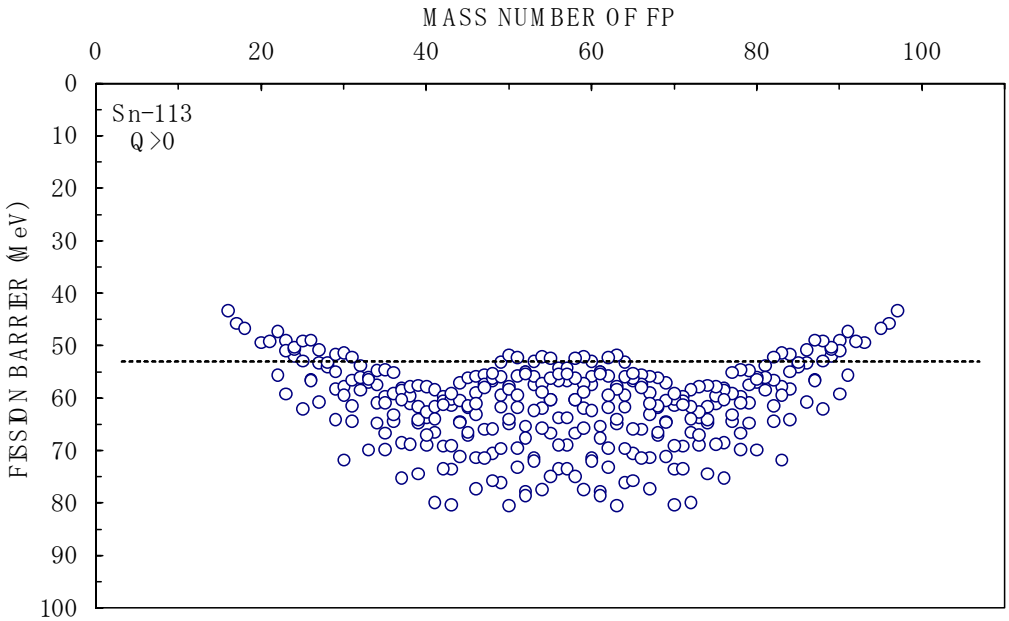

Fig. 5-3: Fission barriers for Sn-113

Slide 40

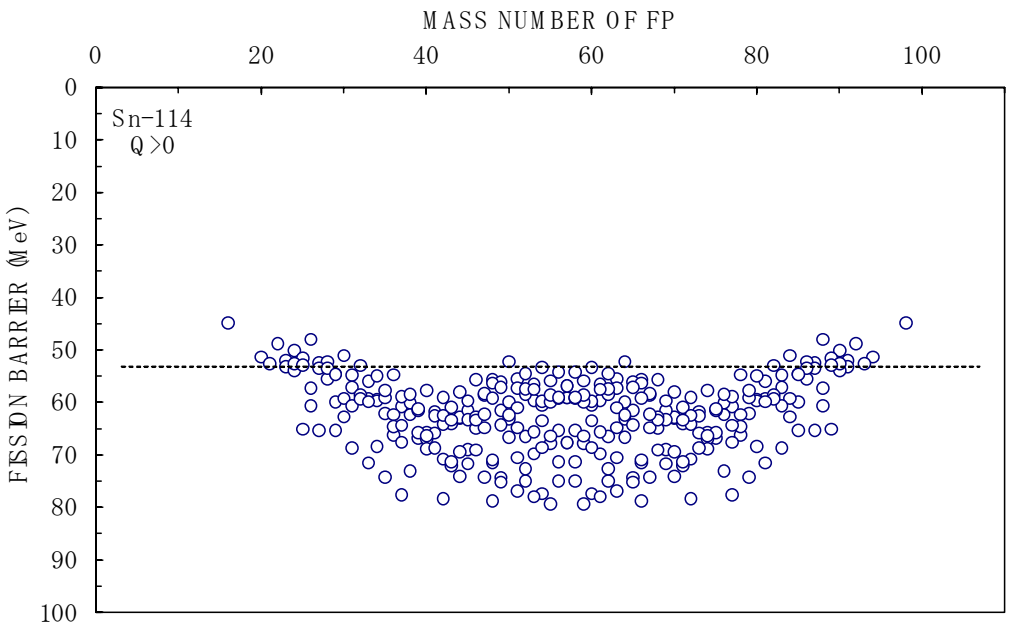

Fig. 5-4: Fission barriers for Sn-114

Slide 41

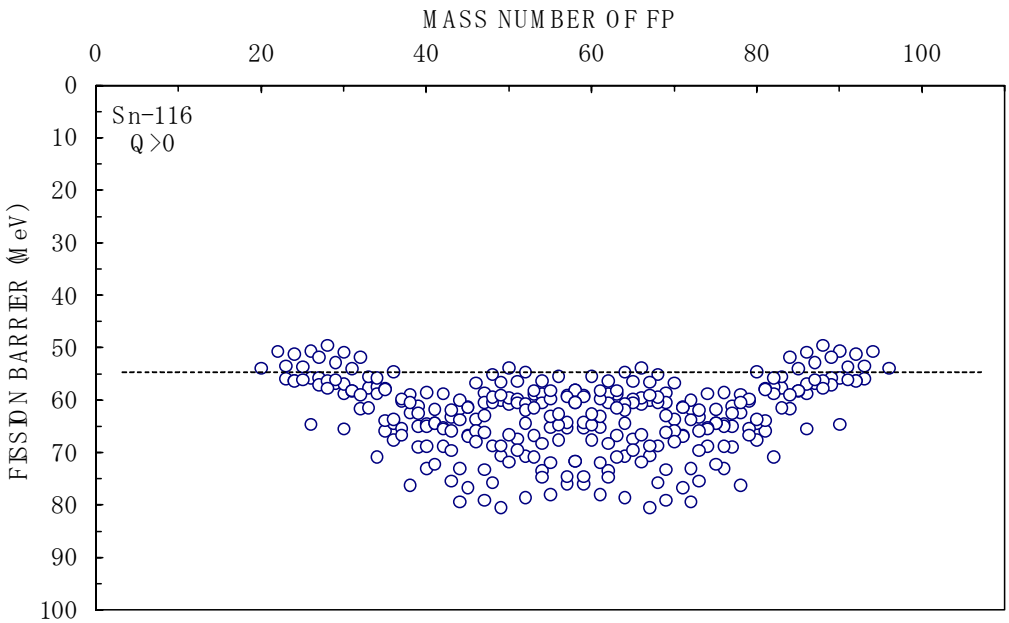

Fig. 5-5: Fission barriers for Sn-116

Slide 42

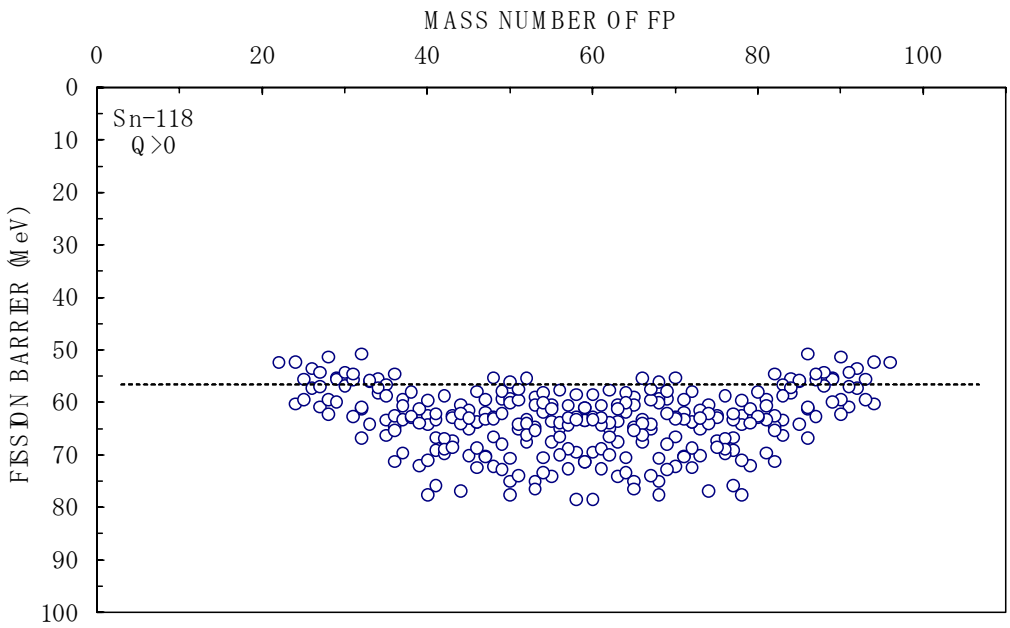

Fig. 5-6: Fission barriers for Sn-118